

Fig. 3 Peak acceleration responses of subsystem for various mass ratios for the STS-41 Z acceleration for $f_1 = 4.6$ Hz.

Sinusoidal Excitation

A typical launch vehicle natural frequency of 5 Hz ($T_l = 0.2$ s) is used as the sinusoidal excitation frequency. The launch vehicle acceleration at the payload support then is given by

$$\ddot{u}_l = 1.56g + 0.5g \sin(2\pi t/T_l) \quad (10)$$

The offset of 1.56g is added to account for the solid rocket booster ignition.

Figure 1 shows the subsystem response spectra for the payload fundamental natural frequency of 4.6 Hz. It is observed that the amplitude of the resonance peak is sharply reduced as the mass ratio increases. In addition, the resonance frequency appears to be somewhat reducing as R_s increases. Figure 2 shows the payload peak acceleration responses for various subsystem frequencies. At the tuning frequency of $f_s \approx 5.0$ Hz, the secondary system behaves as a dynamic-tuned mass energy absorber and the payload spectral amplitudes are reduced by about 40%. For larger f_s , the payload vibration amplitude is generally reduced. It is also observed that larger accelerations are experienced by the payload as mass ratio increases.

Figures 1 and 2 show that the tuning frequency shifts with an increase in mass ratio. The direction of the frequency shift is a function of the ratio of the fundamental natural frequency of the payload to the driving frequency. This trend of variation is consistent with the analytical results described in Ref. 2.

STS-41 ACIP Liftoff Acceleration

In this section, the lift-off accelerations of the STS-41 Aerodynamic Coefficient Instrumentation Package (ACIP) in the Z direction is used. Figure 3 shows the subsystem response spectra for different mass ratios. Additional peaks due to the higher modes of vibration of the payload are also clearly observed in this figure. The response amplitude of the fifth mode is about 75% of that of the first mode. This is because the Z acceleration contains considerable amount of energy at high frequencies ($f_s \geq 30$ Hz). As the mass ratio increases, the resonance peaks for higher modes decrease rather sharply. Additional results concerning effects of damping and STS-41 X acceleration are described in Ref. 2.

Conclusions

The presented results show that a light subsystem may experience much larger loading than its payload. Therefore, structural safety of the subsystem for the liftoff condition must be

carefully analyzed. The subsystem mass ratio has a significant effect on its peak responses for both sinusoidal excitation and STS-41 liftoff ACIP accelerations. The primary-secondary interactions, generally, reduce the peak responses of the subsystem. The amount of reduction increases significantly as the mass ratio increases. The tuning frequency shifts with an increase in mass ratio. The direction of the tuning frequency shift is a function of the ratio of the fundamental natural frequency of the payload to the driving frequency.

Acknowledgments

This work was supported by the National Science Foundation Grant EID-9017559. Many thanks are given to D. Hamilton and J. Dagen from NASA Johnson Space Center and J. Brose and D. Hackler from Lockheed, Software Development Section, for many helpful discussions and supplying the STS-41 flight data.

References

- ¹Su, L., and Ahmadi, G., "Earthquake Response of Linear Continuous Structures by the Method of Evolutionary Spectra," *Engineering Structures*, Vol. 10, 1988, pp. 47-56.
- ²Lee-Glauser, G., and Ahmadi, G., "Dynamic Response Spectra for an Aerospace Payload and Its Attachments," Clarkson Univ., Rept. MAE-232, Potsdam, NY, May 1991.

Earl A. Thornton
Associate Editor

Shaped Discharge Ports for Draining Liquids

K. Ramamurthi* and T. John Tharakan†
Liquid Propulsion Systems Centre,
Valiamala, Trivandrum 695 547, India

Introduction

THE formation of a vortex core during the draining of liquids from tanks not only leads to a reduced outflow but also causes air to be ingested in the discharge. Explicit predictions for the height of the air vortex formed is not possible in free draining situations. The Rankine compound vortex model, which is a combination of free vortex with a forced vortex inside, cannot take into account the axial velocity due to the efflux and the dissipation of vorticity from the core. Dergarabedian¹ has proposed a theoretical model that considers the influence of the efflux on the tangential velocity. However, the analysis is for a liquid that extends to infinity in the radial direction and gives only a qualitative insight into the phenomenon. To evolve the scaling laws for air-vortex formation and hence adopt a scheme to arrest the formation, a series of well-planned experiments were conducted in cylindrical containers with different sizes of drain ports. The results suggest that the incidence of air-vortex formation while draining liquids from tanks can be reduced by suitable shaping of the drain ports.

Rotational motion in the liquid can assist in the formation of vortex. The scaling laws for vortex formation and the effectiveness of shaped ports in suppressing air vortex are studied separately for conditions when 1) the liquid column is initially quiescent and 2) rotational currents are present in the liquid column.

Received April 8, 1992; revision received June 25, 1992; accepted for publication June 29, 1992. Copyright © 1992 by the American Institute of Aeronautics and Astronautics, Inc. All rights reserved.

*Head, Propulsion Research and Studies Group.

†Engineer, Propulsion Research and Studies Group.

Apparatus

The experiments are conducted with water and glycerine filled to different heights in transparent cylindrical tanks of 140, 90, and 30 mm diameter and drained out through cylindrical and shaped drain ports of varying diameters. In some of the experiments, rotational motion is introduced in the liquid column using a stirrer. Fine aluminum powder of 5- μ size is dispersed in the liquid to monitor the circulation currents. The maximum air-vortex heights formed during the draining of the liquid under the different conditions of the experiments are measured for various drain ports.

Scaling of Air-Vortex Heights

Case I: Initial Quiescent Liquid Column

A plot of the maximum air-vortex heights measured in tanks of different diameters discharging through cylindrical ports of varying diameters is given in Fig. 1. The range of port diameters chosen for the experiments spans two orders of magnitude. It is seen that the maximum air-vortex height initially increases monotonically with the drain port diameter and reaches a maximum value after which it rapidly drops to zero. Variations of the initial height to which liquid is filled in the tank does not influence the air-vortex height.

The initially increasing trend of the air-vortex height and rapid drop thereafter is justifiable from physical considerations as follows. For the case of no outflow there can be no vortex. Similarly when the drain port diameter equals the tank diameter, the flow through the port corresponds to that of pipe flow for which there is no possibility of vortex formation.

The results given in Fig. 1 are replotted in Fig. 2 in nondimensionalized coordinates based on the observed dependence of vortex heights on port diameters and tank diameters. Here the measured maximum air-vortex height is divided by port diameter to yield the nondimensionalized air-vortex height. The nondimensional port diameter is taken as the ratio of the measured port diameter to the tank diameter. It is observed that there is considerable scatter in the results. Such a degree

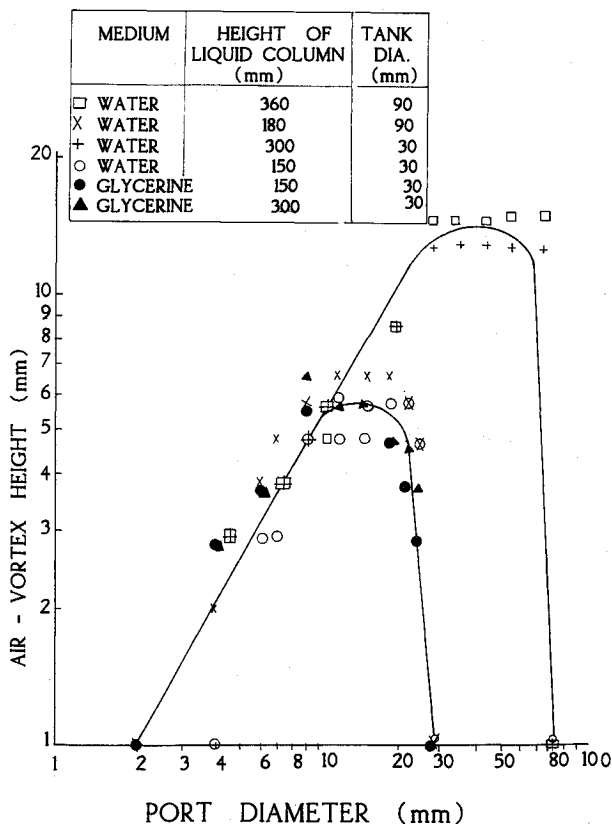


Fig. 1 Maximum air-vortex height for quiescent liquid with cylindrical drain ports.

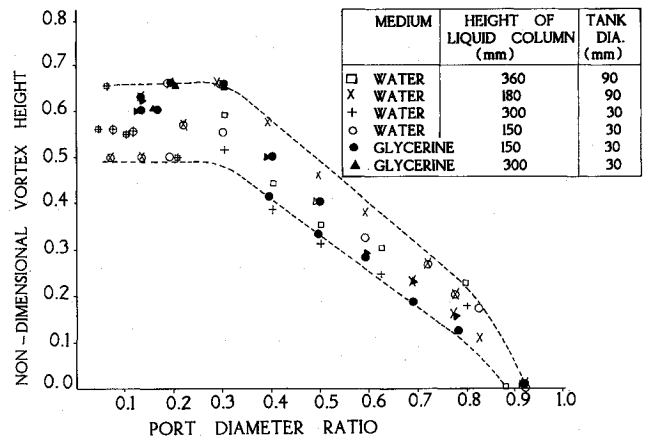


Fig. 2 Nondimensional air-vortex heights with cylindrical drain ports.

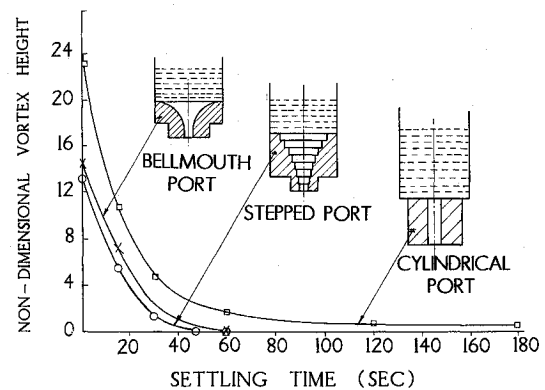


Fig. 3 Air-vortex with cylindrical and shaped ports.

of scatter is also noticed in the experiments of Granger² for relative surge velocities during vortexing. However, the experimental points are well contained within the bounds indicated by the dotted lines. For nondimensional port diameter less than 1/3, the nondimensional vortex height is reasonably constant with values between 0.5 and 0.65. When the port-to-tank diameter ratio becomes greater than 1/3, the nondimensional vortex height decreases and reaches negligibly small values for the port-to-tank diameter ratio exceeding a value of about 0.8.

Case II: Initial Rotational Motion in Liquid Column

The maximum air-vortex heights measured with cylindrical drain ports when the liquid column is stirred at different speeds show additional dependence on the initial height to which the liquid is filled in the tank. With rotational motion in the liquid, a higher liquid column gives an enhanced air-vortex height for smaller port diameters. Such a trend for rotating liquids has also been seen in the investigations of Dodge³ wherein, for small discharge ports, lower discharge coefficients and reversal of axial velocities close to the air core have been observed. However, for drain port diameter ratios exceeding about 0.3, a lower height of liquid column gives rise to a larger air vortex. This appears reasonable since with the smaller liquid column the rotational motion is transferred more effectively over the depth of the liquid augmenting vortex formation.

When the initial rotational velocity in the liquid column is decreased, the air-vortex height also drops. The air-vortex heights show a stronger dependence on height of the liquid column for larger rotational velocities in the liquid. The scaling laws for air-vortex heights in the presence of rotational motion in the liquid therefore become complicated with the additional dependence on liquid column height and the dissipation of rotational velocities by the walls of the tanks. How-

ever, at large port-to-tank diameter ratios, the formation of vortex is hindered as observed for initial quiescent conditions in the liquid. This appears justifiable due to nearly pipe flow conditions at the entrance to the drain port at the large port diameter ratios.

Shaping of Discharge Ports

Shaped ports can be configured to give a gradual reduction in diameter from the tank to the outlet of the drain port. Such shaped ports can be either in the form of a stepped port with the diameter reduction in successive steps or as a bellmouth. The bellmouth can have a circular shape and has been considered by Binnie and Hookings.⁴ Figure 3 shows these shaped ports and their performance. In view of the successive reduction in diameters, these shaped ports bring about a small reduction in diameter as the flow enters and progresses in the drain port. This yields locally large values of port diameter ratios. Based on the results of experiments with cylindrical ports, a drastic reduction in air-vortex heights is to be anticipated with their use.

The air-vortex heights measured with the stepped, bellmouth, and cylindrical drain ports of the same exit diameter are compared in Fig. 3. These heights are measured at different times after stopping the stirrer that induces forced rotation of the liquid. The time between stopping of the stirrer and starting the draining is called settling time. A larger settling time denotes a lower level of rotational velocities in the column of liquid since with increasing settling time the rotational currents get dissipated. For times exceeding 5 min the liquid column becomes fully quiescent. It is seen that, with the stepped configuration of drain port, the vortex height becomes zero at very small settling times. The stepped port is therefore very effective in arresting vortex formation even when rotational motion is present in the liquid column. The bellmouth port also reduces the height of the maximum air vortex; however, it is not as effective as the stepped drain port. The cylindrical drain port gives the largest height of air vortex that persists even when all rotational flow velocities in the liquid column are dissipated.

When large rotational velocities are present in the liquid column (small values of settling time in Fig. 3), the shaped ports do not totally suppress the formation of air vortex as under initial quiescent conditions. A combination of vortex-arresting baffles that dissipate the rotational motion in the

liquid and the shaped drain ports discussed here can therefore completely eliminate the formation of air vortex during the draining of liquids from tanks.

References

- ¹Dergarabedian, P., "The Behaviour of Vortex Motion in an Emptying Container," *Proceedings of the 1960 Heat Transfer and Fluid Mechanics Institute*, Stanford Univ., Stanford, CA, 1960, pp 47-61.
- ²Granger, R. A., "Speed of Surge in a Bathtub Vortex," *Journal of Fluid Mechanics*, Vol. 34, Dec. 1968, pp. 651-656.
- ³Dodge, F. T., "Dynamic Behaviour of Liquids in Moving Containers with Application to Space Vehicle Technology," NASA SP-106, 1966.
- ⁴Binnie, A. M., and Hookings, G. A., "Laboratory Experiments on Whirlpools," *Proceedings of Royal Society of London, Series A, Mathematical and Physical Sciences*, Vol. 194, Sept. 1948, pp. 398-415.

Errata

Low Earth Orbit Simulation and Materials Characterization

R. A. Synowicki, Jeffrey S. Hale,
and John A. Woollam
*University of Nebraska at Lincoln,
Lincoln, Nebraska 68588*

[JSR Vol. 30, No. 1, pp. 116-119 (1993)]

IN the original publication, two errors were inadvertently introduced in the title and author lines. They appear correctly above.